



REMOTE SENSING OF ICE AND SNOW BY COMPACT RAMAN LIDAR

V.N. Lednev¹, S.M. Pershin¹, R.N. Yulmetov^{1,2}, A.F. Bunkin¹

¹Wave Research Center of Prokhorov General Physics Institute RAS, Moscow, Russia

²The University Centre in Svalbard, Longyearbyen, Norway

ABSTRACT

Compact Raman LIDAR system for remote sensing of sea, snow and ice was developed in Wave Research Center at Prokhorov General Physics Institute of RAS. Diode pumped solid state laser (532 nm, 5 ns, 200 μ J/pulse, 1 kHz) in combination with grating spectrograph equipped with gated detector (ICCD) resulted in high sensitive detection in wide spectral range. Light weight (~20 kg), small dimensions and low power consumption (~200 W) make it possible to install such system on any vehicle including unmanned submarine or aircraft system.

The lidar was used for remote detection of water and ice temperature on the basis of Raman scattering of water molecules.

The express ice thickness measurement technique by remote sensing methods with the mm accuracy have been suggested by comparison of elastic and Raman scattering.

The snow characterization by compact LIDAR system has been carried out. Several signals were measured to indicate difference in snow properties: elastic scattering, Raman spectroscopy, fluorescence of organic compounds. A simple technique for classification of different types of snow (fresh snow, snow cover, old snow) has been proposed.

The perspectives of compact LIDAR systems for express under satellite monitoring of ice and snow for ecology applications and Global climate changes studies in Arctic region are suggested.

INTRODUCTION

The interest to the research in the Arctic Ocean and polar areas has been increasing in the last decades for two reasons: oil and gas production and global climate changes monitoring. Continuous diagnostics of human activity influence on the ecology and global climate changes are the most pressing goals for research in all countries located in the Arctic region. Depending on the research goals different techniques can be used for laboratory measurements while monitoring of vast areas can be carried out only by remote sensing (Bunkin, 2001; Measures, 1984). Human activity influence on ecology can be traced by pollution detection: oil, chemicals or heavy metals in the ocean water. Global climate change is studied on the basis of the temperature and chlorophyll distribution in the Arctic Ocean using remote methods: spaceborne radars (Johannesson, 1999), airborne microwave and laser scatterometers (Remund, 1999; Measures, 1984).

The Arctic Ocean is an excellent region for revealing climate changes and at the same time the Arctic Ocean has a strong influence on the climate. In the northern regions, the ice study is of the great interest due to the fact that ice serves as an effective interface between the ocean and the atmosphere, restricting exchange of heat, mass, momentum and chemical constituents. Detailed study of the global climate system and prediction of future climate changes can be made only if reliable data on different physical parameters of water and ice are available.

These parameters include water and ice temperature, salinity, ice surface roughness, optical and thermodynamic properties of the snow cover, and the presence of liquid water above ice, which frequently occurs in summer when ice and snow melt at the ice surface.

Conventional techniques for temperature detection include spaceborne radiometer radars, airborne microwave and laser scatterometers. However, temperature detection by satellite radiometer is performed in a thin 30 μm surface layer of seawater. It was found that under low speed wind conditions the temperature of surface layer was by 0.5 – 1 $^{\circ}\text{C}$ lower than in the water column (Soloviev, 1987). The temperature detected by radars can be strongly influenced by surface waves. Frazil or grease ice can significantly change the results of measurements with such techniques in the Arctic region. Specifically, in the first stage of freezing small ice crystals are formed at the surface and as the freezing continues the crystals coagulate and form frazil ice. This frazil ice damps the short gravity waves at the sea surface, which has significant impact on radar remote sensing of the open ocean water.

The Raman spectroscopy is a promising method for remote detection of water temperature. This method has been successfully used by different scientific groups both in laboratory (Pershin, 2010; Walrafen, 1986, Sun, 2009) and field experiments (Lee, 2002; Bunkin, 2011). Additionally, any system for Raman spectroscopy is based on the laser source that can be used as a source of excitation for chlorophyll or organic matter fluorescence. The Raman systems for remote sensing can be used for monitoring of several parameters simultaneously: water temperature, chlorophyll and distributed organic matter (DOM), sea water contaminations by gas or oil production activity. Two approaches can be used for remote detection of water temperature by the Raman spectra, i.e. by fitting of OH-band profile of Raman spectra for bulk water (Sun, 2009) and OH-band profile center correlation on temperature (Pershin, 2010). The accuracy of temperature detection by the fitting method is generally about 1 $^{\circ}\text{C}$. The second procedure was developed by our group; it can be characterized by improved temperature accuracy detection that is better than 0.5 $^{\circ}\text{C}$. Ice temperature can be also detected by the Raman spectroscopy but the error will be higher.

Raman systems can be installed on airborne platforms that would be especially useful for express diagnosis of large areas in any region including hardly accessible areas like the Arctic Ocean or mountain lakes. If gated detector is used for signal digitizing then range resolved study can be carried out including depth profiling of temperature, chlorophyll or organic matter distribution. Recent progress in laser technologies and high-speed electronics give opportunity to develop compact system for ranged Raman measurements (Bunkin, 2012). Small mass and compact size of such systems provide a possibility to install these devices on aircrafts or submarines including remotely driven platforms that can be extremely useful for Arctic exploration.

EXPERIMENT

The LIDAR system was developed at the Wave Research Centre of the Prokhorov General Physics Institute of the RAS and is presented in the Fig. 1. The LIDAR is based on a compact diode pumped solid state YVO₄:Nd laser (Laser Compact, Ltd., model LCM-DTL-319QT: 527 nm, 5 ns, 1 kHz, 200 $\mu\text{J}/\text{pulse}$). Beam diameter at $1/e^2$ level at the laser output is estimated at 1.8 mm, the beam divergence is 0.8 mrad. Two prisms were used to align the probe laser beam and optical path of the receiving channel. Signals from a remote object were collected by a quartz lens ($F = 21$ cm, diameter 9 cm) and directed by an aluminum coated mirror ($l \times h$ 4x3 cm) to the input slit of the spectrograph. Signal collecting efficiency was estimated in the air by elastic scattering from concrete wall at 12 m distance by spot diameter at the spectrograph slit and its value was ~ 250 μm . The band-pass glass filters were used to suppress scattered laser radiation. Detection system consists of compact spectrograph (Spectra

Physics, MS127i) equipped with gated detector (intensified CCD or ICCD, Andor iStar). We used low resolution grating 150 lines/mm and slit width 250 μm to increase signal-to-noise ratio. Spectral resolution was 120 cm^{-1} that was detected by measuring of FWHM (full width at half maximum) for scattered laser line. The chosen spectral window was 500 - 750 nm that made possible to register several signals simultaneously. The echo-signal is a sum of Mie, Rayleigh (527 nm), Raman (OH-bond center 650 nm) scattering, fluorescence from organic components (600 nm) and chlorophyll "a" (685 nm). The signals for elastic and Raman scattering, fluorescence were determined as the integral of the corresponding band with background correction. The ICCD detector allowed us to obtain gated images with 5 ns duration and 0.25 ns step. The time jitter between laser pulse and detection gate was less than 3 ns that provided a depth resolution of 0.85 m (the column high was 0.55 m with an error of 0.31 m) for underwater measurements. In all experiments we used a gate of 5 ns. Time - of - flight spectra measurements were carried out by varying the delay between laser pulse and exposure gate. The gated detection effectively suppressed background sun irradiance scattered by seawater. The system was limited to low repetition rate 23 Hz due to the maximum detector digitizing rate. The experimental setup was controlled by a PC and the software allows us to perform automatic measurements depending on the goal: sea depth profiling or mapping study. Light weight (~ 20 kg), small dimensions (60x40x20 cm) and low power consumption (~ 300 W) make it possible to install such system on any vehicle including unmanned aircraft system.

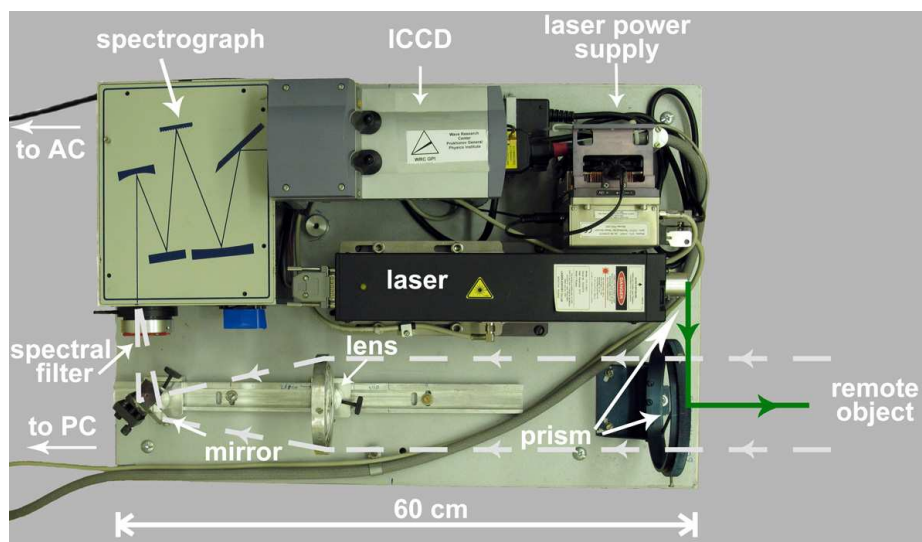


Figure 1. Compact Raman LIDAR system developed at WRC GPI.

Laboratory experiments

A typical spectrum of the seawater sample measured at distance of 5 m is presented in Fig. 2. The spectrum (Fig. 2) is a sum of the Mie, Rayleigh scattering, Raman scattering, fluorescence from dissolved organic material and phytoplankton (chlorophyll).

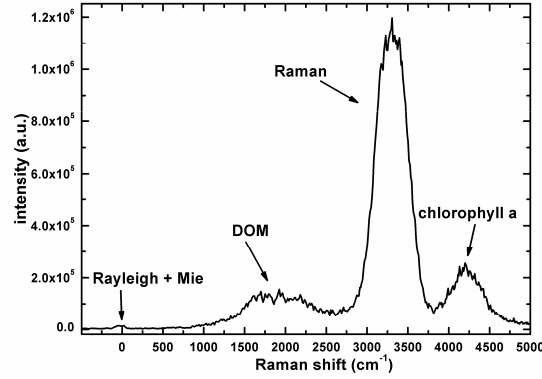


Figure 2. The typical spectrum of seawater: Mie and Rayleigh scattering (527 nm), Raman scattering (OH-bond center 650 nm), fluorescence from organic components (600 nm) and chlorophyll "a" (685 nm).

Temperature measurements

Previously we have proposed a method for remote temperature detecting based on Raman spectrum of water OH-band (Pershin, 2010). The tank with a volume of 1.5 m^3 was filled with the seawater and under controlled temperature conditions Raman spectra was detected. Laser beam was directed vertically into the tank by an aluminum coated mirror placed 1 m above the water surface. The detection system was placed in another room and the spectra were collected through a glass window. The length of optical path from laser output to water surface was about 5 m. The Raman spectra were detected at different temperatures of both seawater and distilled water. According to the suggested procedure (Pershin, 2010) every spectrum was fitted with the Gaussian profile (Fig. 3a) for different temperatures. The centers of fitted curves were plotted versus temperature for calibration of LIDAR (Fig. 3). It should be noted that the suggested procedure is very sensitive to profile variations and can be effectively used for remote temperature study. In our first paper we have compared the temperature detected by our system and by a thermocouple. The differences were within a range of $0.5 \text{ }^\circ\text{C}$ that was estimated as the error of this technique. In the case of compact LIDAR the results were poorer and the accuracy was about $1 \text{ }^\circ\text{C}$ (Fig. 3). The slopes of curves for seawater and distilled water differed by 18%. The water salinity should be known for reliable detection of water temperature by Raman spectroscopy. The same problem arises in the detection of temperature by fitting of OH-band profile (Sun, 2009).

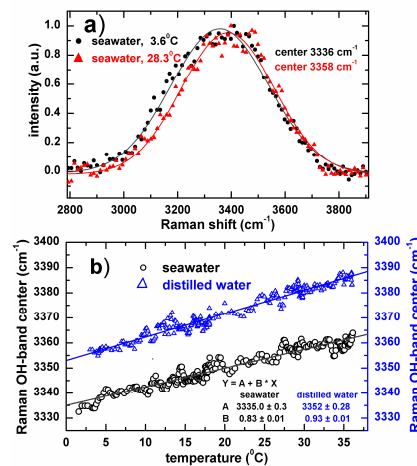


Figure 3. System calibration for temperature detection by Raman spectroscopy.

- Raman OH-band fitted with the Gaussian profile for seawater at different temperatures;
- Raman OH-band centers versus temperature for distilled water and seawater.

The Raman spectrum for water and ice have different OH-band profile (Fig. 4) which is perspective for ice thickness measurements by optic techniques.

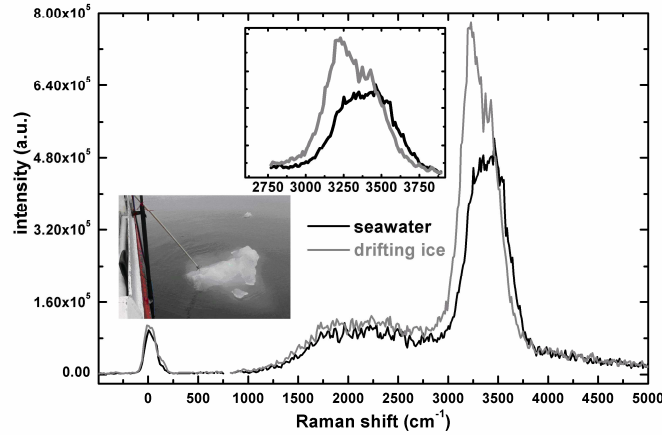


Figure 4. The Raman spectra of ice and water (OH-band profile is presented in the insert).

Ice thickness measurements

The capabilities of the Raman spectroscopy for ice thickness measurements by remote sensing were demonstrated for the fresh ice sample. The distilled water of 5 litres was freeze during 20 hours at temperature of -20°C to form a fresh ice. Than sample was taken into tank filled with distilled water. The lidar system was installed 5 m away from the sample. A quartz lens ($F = 120\text{ mm}$) installed in a movable stage was placed several centimetres above floating ice. The detected spectrum contains both elastic and Raman scattering signals that were used for ice thickness measurements. Ice absorption is low in the spectral range of our interest (absorption coefficient is 0.28 m^{-1} for wavelength equal to 650 nm) so ice absorption could be ignored for ice thickness below 0.5 m. In our experiments, the ice thickness was 97 mm and can be assumed to be optically thin. The spectrum can be described as a combination of ice and water spectrum. The spectra were taken at different position of lens to sample distance. For upper edge measurement of floating ice the elastic scattering can be a good choice since difference in refraction index between air and ice is significant. But this signal can't be used for bottom edge ice determination since difference of refractive index for water and ice is less than 0.03. The differences in the Raman OH-band profile can be used for ice thickness measurements. A center of OH-band profile was plotted vs. lens distance that corresponds to different regions of laser spot and the results are presented in the Fig. 5.

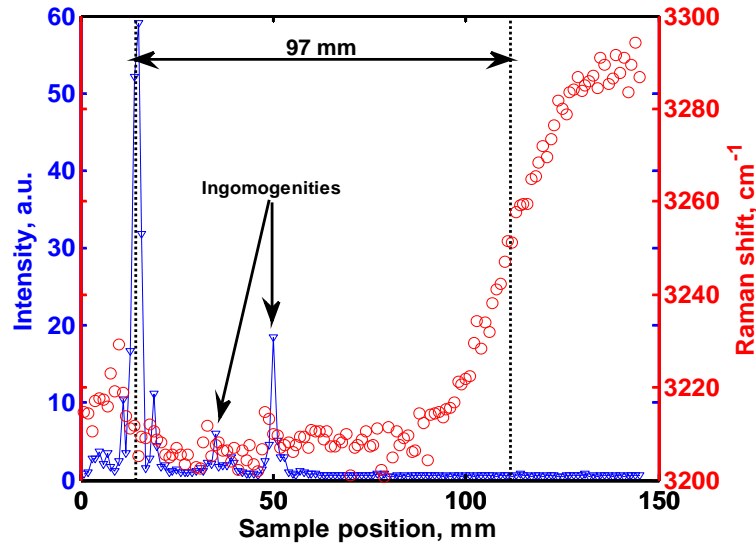


Figure 5. Ice thickness measurements by Raman spectroscopy. The ice top is found by elastic scattering (blue), ice bottom is determined by Raman OH-band center shift (red) in region of ice and water.

Field experiments

Snow characterization

The snow is unique material that strongly affects sunlight absorption and thermodynamics of polar areas. Our study was devoted to estimate capabilities of Raman spectroscopy for snow remote sensing and to find out differences of fresh and cover snow. A snow sample was taken 1 hour after snowfall in Moscow on 5 April, 2012. One week before there were large temperature fluctuation that formed a snowcover. A comparison of the Raman spectra for fresh, cover and old snow is presented in the Fig. 6. Spectra were taken from the top view of the sample. Spectra were spatially averaging during measurements by sample movement. For the fresh snow sample a 1 mm thick layer was removed by knife just before experiment to prevent snow melting influence on the results. Then fresh snow was removed to expose snow cover and the same way was made for old snow. Snow types differed significantly by reflectivity that is widely used in snow classification by scattering techniques. Raman signal (OH-band profile) was 20-50 times lower compared to liquid water or ice samples due to effective elastic scattering of snow. similar for three types of snow but definite distinct features can be pointed out according to presented figure. Old snow spectra can be characterized as classic ice sample spectrum. For snow cover spectra intensity was greater for the band at 3300 cm^{-1} . The Raman spectrum for fresh snow was a water type spectrum. For the ensure that this is not due to snow melting a several times 1 mm layer was removed and spectra was detected during 20 sec but no changes were observed for fresh snow. Raman signal is proportional to laser pulse energy and concentration of water molecules. A ratio of elastic to Raman signals can be used to characterized remotely snow density. Density of fresh and old snow was estimated by conventional method and was 0.12 and 0.45 s respectively. The elastic to Raman ratios was 0.12 and 1.1 respectively so it can be used for remote detection of snow density.

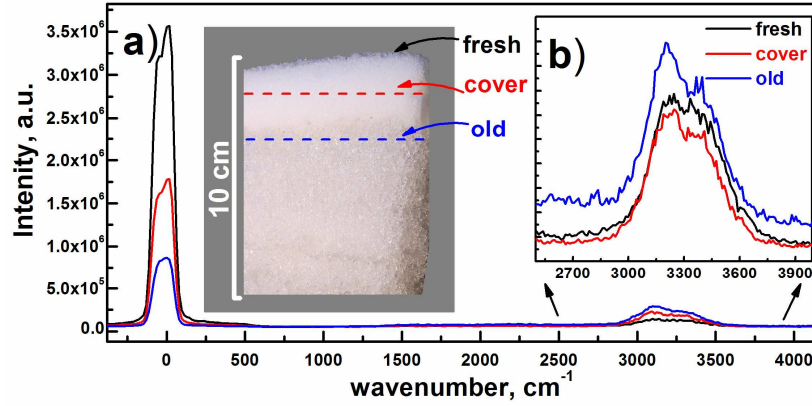


Figure 6. Raman spectra for different snow layers (a) and detailed OH-band (b):
fresh snow (black), snow cover (red) and old snow (blue).

The snow sample was used for depth profile study to compare snow age with the measured signals and results are presented in the Fig. 7.

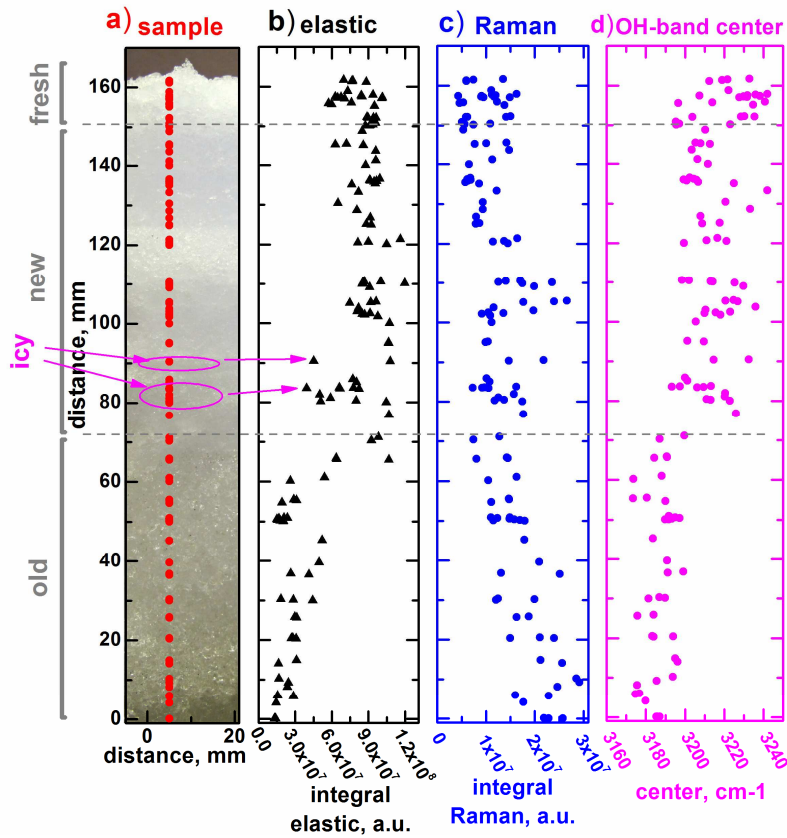


Figure 7. Snow depth profile measurements by Raman spectroscopy:

- a) snow sample and sampled points (red round); b) elastic signal at depth profile (black triangle);
- c) Raman signal at depth profile (blue round); d) Raman OH-band center at depth profile (magenta round).

Snow sample was taken on 23 March 2012 and was placed in laboratory during 5 minutes before measurements and every 2 minutes a 1 mm thin layer was removed to fresh surface. A size of the area that was used for measurements were about 1 mm diameter round to obtain spatial averaging to decrease influence of snowflakes and particle sizes.

Perspectives

Compact Raman system for remote sensing of ocean is of growing interest since these systems can give reliable information about water temperature, water contaminations and chlorophyll concentration in locations that can hardly be accessed (Arctic region or mountain lakes).

One of the possible applications is to study the iceberg evolution during its motion in the open ocean. Direct measurements of iceberg parameters, i.e. temperature, salinity, mechanical properties of ice, dimensions are difficult and dangerous to perform. If a compact system will be installed on remotely operated aircraft then properties of iceberg and surrounding water can be traced automatically and safely. Laser ranging with excitation laser from the Raman system can be used to measure iceberg form and size for above and under water parts with a resolution below 5 cm. The temperature of iceberg and surrounding water can be remotely detected by Raman spectroscopy of OH-band profile that are of great importance for the study of iceberg thermodynamics. The Rayleigh, Mie and Raman scattering can reveal different ice properties as porosity, salinity, and density of ice. Additionally iceberg melting evolution and its influence on nearby seawater can be studied in detail with remotely driven LIDAR system. This study can indicate perspective procedures for express simple detection of icebergs for safe sailing in the northern seas.

Compact system can be installed on stationary platform in the Arctic Ocean as a real time automatic alarm service to detect approaching icebergs. Laser ranging can be used for mapping sea surface and automatic detection of floating objects which can be dangerous for the platform. Raman spectroscopy can be used to validate that floating object is ice. Additionally such system can be also used for express diagnostic of oil leaks at early stages in immediate vicinity of the platform.

Combination of compact Raman system and remotely operated ship or submarine can be used for automatic detection of water properties along an arbitrary path in any place of interest. These data can improve the satellite data reliability for the temperature distribution for detecting global climate changes.

CONCLUSIONS

Remote sensing in the Svalbard fjords was carried out by compact LIDAR system. The system has small weight (~ 20 kg) and low power consumption (< 200 W) and can be installed on any vehicle including remotely operated submarine or aircraft. The Raman spectroscopy was used for remote temperature detection of water. The capabilities of Raman spectroscopy for remote detection of ice thickness were estimated. The snow characterization by Raman spectroscopy has been performed. The developed system was used for remote sensing of large sea regions: bulk water temperature, chlorophyll and dissolved organic distribution mapping for surface and depth profiling applications. Possible applications of the compact Raman LIDAR for express monitoring of seawater properties in the places with high concentration of floating ice in the ocean are discussed.

Study was partially supported by RFBR grants 11-02-00034-a, 11-02-01202-a and 12-02-31398-mol_a.

REFERENCES

Bunkin A.F., Voliak K.I., 2001, Laser Remote Sensing of the Ocean. Methods and Applications. John Wiley&Sons, Inc. New York, Chichester, Weinheim, Brisbane, Singapore, Toronto, 244 pp.

Bunkin A.F., *et.al.*, Ship wakes detection by Raman LIDAR, *Applied Optics*, **50**, 86-89 (2011)

Bunkin A.F., *et.al.*, Remote sensing of seawater and drifting ice in Svalbard fjords by compact Raman lidar, *Applied Optics*, **51**, 5477-5485 (2012)

Johannessen O. M., *et.al.*, Satellite evidence for an Arctic sea ice cover in transformation. *Science*, **286**, 1937–1939 (1999)

Lee K.-J., *et.al.*, Helicopter-Based Lidar System for Monitoring the upper Ocean and Terrain Surface, *Applied Optics*, **41** (3), 401-406, (2002)

Measures R.M., 1984, Laser Remote Sensing. Fundamentals and Applications. John Wiley & Sons. New York, Toronto, Singapore, 510 pp.

Pershin S.M., *et.al.*, Evolution of the spectral component of ice in the OH band of water at temperatures from 13 to 99°C, *Quantum Electron*, **40** (12), 1146–1148 (2010)

Soloviev A.V. and Lukas R., Observation of large diurnal warming events in the near-surface layer of the western equatorial Pacific warm pool, *Deep-Sea Research*, **44**, 1055-1076, (1997)

Sun Q., The Raman OH stretching bands of liquid water, *Vibrational Spectroscopy*, **51**, 213 – 217 (2009)

Remund, Q. P. and D. G. Long. Sea ice extent mapping using Ku-band scatterometer data. *J. Geophys. Res.*, **104** (C5), 11515–11527. (1999)

Walrafen G.E., *et.al.*, Temperature dependence of the low - and high - frequency Raman scattering from liquid water, *J. Chem. Phys.* **85**, 6970 - 6983 (1986)